

## Dielectrophoretic tweezers for examining particle-surface interactions within microfluidic devices

Sang Woo Lee<sup>a)</sup>

*Department of Biomedical Engineering, Yonsei University, Heungup Wonju, Gangwondo 220-710, Korea*

Haibo Li

*SanDisk Corporation, 601 McCarthy Blvd. Milpitas, California 95035*

Rashid Bashir<sup>b)</sup>

*Birck Nanotechnology Center, School of Electrical and Computer Engineering and Weldon School of Biomedical Engineering, Purdue University, West Lafayette, Indiana 47907*

(Received 22 January 2007; accepted 8 May 2007; published online 30 May 2007)

The authors present dielectrophoresis (DEP)-based tweezers that can be used to characterize the interactions between a particle and the surface it is attached to, within a microfluidic device. As a proof of concept, 5.4  $\mu\text{m}$  polystyrene beads functionalized by carboxyl group were attached on a bare and poly-L-lysine functionalized oxide surface. Negative dielectrophoresis force was generated using interdigitated electrodes and the peak dielectrophoresis voltage where the beads were repelled away from the surface was used to characterize the strength of interaction between the particle and the surface. Electric field and DEP force calculation were used to corroborate the measured results. © 2007 American Institute of Physics. [DOI: 10.1063/1.2744483]

The characterization of biological interactions such as DNA hybridization, ligand-receptor interactions, and antigen-antibody binding is critical in all aspects of biology and medicine. In spite of the fact that this information is critical to many applications, there have been only a few reports of techniques which allow the possibility of direct measurement of these binding forces. The most prominent approaches include the use of atomic force microscopy (AFM),<sup>1-4</sup> the use of optical tweezers or traps,<sup>5-7</sup> and the use of magnetic tweezers.<sup>8-10</sup> For the case of AFM, one molecule is attached to a surface and the other to the tip of an AFM. The functionalized tip is brought close to the surface allowing the two molecules to interact and then the tip is retracted while measuring the forces required for breaking the bonds between the two molecules. The “laser tweezer” approach relies on the manipulation of functionalized microparticles, which are brought close and then pulled apart, using the forces induced on the particles by the laser, to examine the forces of interaction. These techniques can analyze single particle interactions but are difficult to perform on many particles simultaneously. For the case of magnetic tweezers, magnetic beads attached to molecules are allowed to interact with a functionalized surface and then removed from the surface by applied magnetic force. As a result, the characteristics of biological molecules can be extracted from the analysis of the interaction. However, the implementation to create repulsive interaction between the magnetic beads and the functionalized surface is complicated. In this letter, we report a new approach called “dielectrophoresis tweezers,” which can be used to characterize and manipulate particles attached on an insulator surface by various biological interactions. The approach described can be used within a microfluidic device in an integrated manner using built-in electrodes, which can generate a repulsive force between the

particles and the electrodes due to negative dielectrophoresis.

The dielectrophoresis tweezers were fabricated with a metal interdigitated (IDT) electrode array on an oxidized silicon substrate using lift-off techniques, where the metal lines were 40  $\mu\text{m}$  wide with 20  $\mu\text{m}$  space. The metal layer consisted of 200 Å thick titanium layer and an 800 Å thick platinum layer, which were deposited sequentially in a sputtering system. A 4000 Å thick plasma-enhanced chemical-vapor deposition oxide layer was then deposited on the wafer. An untreated surface and surface treated with poly-L-lysine were used for the experiments. In order to form a poly-L-lysine self-assembled monolayer on the oxide surface, we used the following sequence of steps: (1) A chip having the IDT array covered by the oxide were cleaned in acetone and methanol, rinsed in a solution of 20 ml H<sub>2</sub>O, 30 ml ethanol, 5 g NaOH, and then rinsed in de-ionized (DI) water thoroughly. (2) The chip was then cleaned using an oxygen plasma for 20 min. (3) 200  $\mu\text{l}$  poly-L-lysine (Sigma P-6282) solution at concentration of 0.1 mg/ml was introduced into the chip and incubated for 1 h at 37 °C. (4) The chip was rinsed with DI water and dried by nitrogen. A polydimethylsiloxane (PDMS) layer with 1 mm thickness was then used to form a reservoir over the chip. Commercially available 5.4  $\mu\text{m}$  diameter polystyrene beads functionalized with carboxyl groups (Spherotech Inc., CP-50-10, the original concentration of the stock solution was  $1.1 \times 10^8$  #/ml and was diluted to  $5 \times 10^4$  #/ml with DI) were introduced onto the chip with a bare oxide surface or a poly-L-lysine functionalized oxide surface. The conductivity of the DI water solution containing the beads was  $1.5 \times 10^{-4}$  S/m. Subsequently, a glass slide was used to cover the top of PDMS reservoir. The beads were allowed to settle and interact with the surface and after 5 min, a sinusoidal signal at 1 MHz with varying peak voltages was applied using micromanipulator probes to the IDT pads. At this frequency, the particles experience negative dielectrophoresis (DEP), i.e., the particles move away from the regions of the highest field gradient since the Clausius-Mossotti factor,  $\text{Re}[K(\omega)] = \text{Re}[\tilde{\epsilon}_p - \tilde{\epsilon}_m / \tilde{\epsilon}_p + 2\tilde{\epsilon}_m]$  is negative,

<sup>a)</sup>Electronic mail: yusuklee@yonsei.ac.kr

<sup>b)</sup>Electronic mail: bashir@purdue.edu

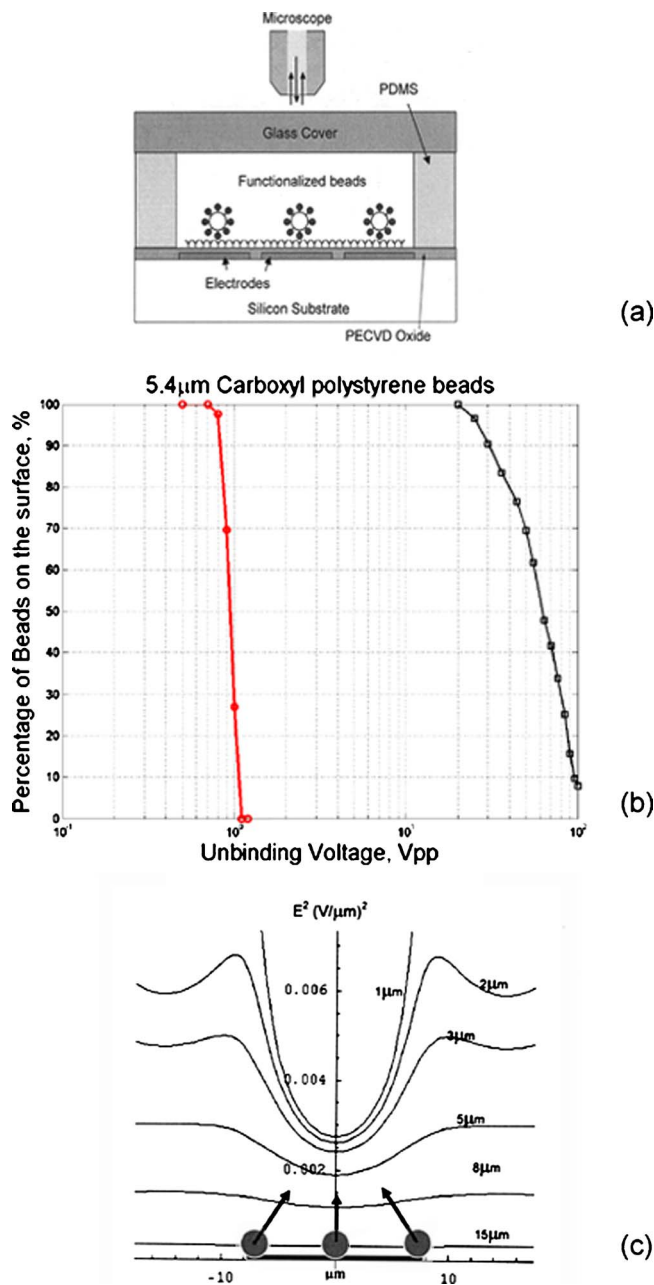


FIG. 1. (Color online) (a) Schematic diagram of the experimental setup (drawing not to scale). (b) Average measured percentage of 5.4 μm diameter carboxyl coated beads in contact with the uncoated or the poly-L-lysine functionalized surface at the center of the electrode as the function of voltage after five measurements (variation is less than 10%). (c) Simulation results of the electric-field square for an IDT metal electrode (see Ref. 11) and schematic diagram of negative DEP acting on the beads at the surface. Beads at the edges and center of the electrodes would be pushed away.

where  $\tilde{\epsilon}_p$  and  $\tilde{\epsilon}_m$  are complex permittivities of the microbeads and the medium, respectively (bulk conductivity and permittivity of polystyrene bead =  $2.4 \times 10^{-4}$  S/m and  $2.6\epsilon_0$ , permittivity of DI water =  $78\epsilon_0$ ). With the microscope objective focused on the oxide surface, the peak voltage was increased in small increments until the beads were repelled away and removed completely from the unfunctionalized or functionalized oxide surface above the IDT electrodes. Optical micrographs were taken to count the beads present at each voltage step. Figure 1(a) shows the schematic diagrams of the experimental setup. The measured percentage of beads at the center of the electrode located on the oxide

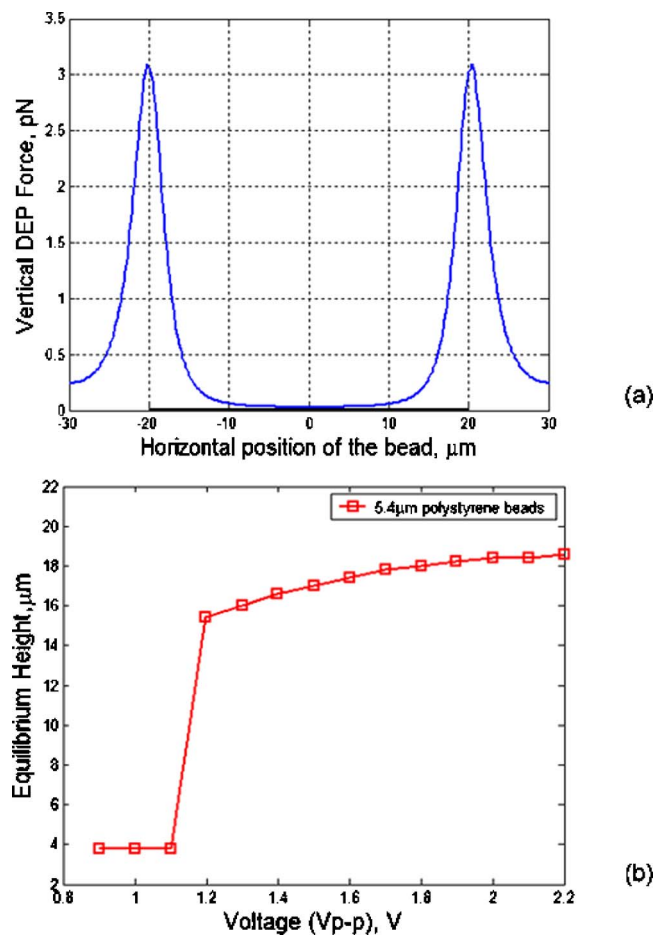


FIG. 2. (Color online) (a) Calculated vertical DEP force at the height of the center of particles with  $R=2.7 \mu\text{m}$  located on the oxide surface (thickness =  $0.4 \mu\text{m}$ ) above the center of electrode. (b) Calculated equilibrium height of the bead as the function of applied voltage. The value of  $\sim 1.1$  V is close to the voltage at which all beads have lifted off from the center of the electrodes, shown in Fig. 1(b) as lines with circles.

with the unfunctionalized (circles) and the functionalized (squares) surfaces as a function of applied voltage is shown in Fig. 1(b).

As shown in Fig. 1(c), negative DEP forces inside IDT electrode structures move the beads away from the regions of the highest electric-field gradient. As can be noted, only a vertical (in  $y$  direction) DEP force acts on the beads located at the center of the electrodes. The force can be estimated by modeling based on the experimental parameters as follows: (1) The total DEP force<sup>12</sup> is given by  $\mathbf{F}_{\text{total}} = \sum_0^{\infty} -\nabla U_n$ , where  $n$  is the force order, and  $U_n = -[2\pi\epsilon_m K_n r^{(2n+1)} / (2n+1)!!] \times \sum_{i+j+k=n} (1/i!j!k!) [\partial^i \Phi / \partial x^i \partial y^j \partial z^k]^2$ , where  $\Phi$  refers to electrostatic potential of the external electric field, and  $K_n = n(2n+1)(\tilde{\epsilon}_p - \tilde{\epsilon}_m) / [n\tilde{\epsilon}_p + (n+1)\tilde{\epsilon}_m]$  is the  $n$ th-order Clausius-Mossotti factor. Based on this equation, a MATLAB (R12, Mathworks) code was developed for calculating the total DEP force. (2) Electrical-field profiles above the IDT electrodes with  $40 \mu\text{m}$  width and  $20 \mu\text{m}$  spacing, when the ac signal with 1 V<sub>peak-to-peak</sub> and 1 MHz was applied to the electrodes, were generated from a finite element program (version 5.7, ANSYS Inc.) with a grid spacing of  $0.2 \mu\text{m}$ . (3) The experimental parameters and the generated electric-field data were used as inputs for the MATLAB code. Figure 2(a) shows the simulated vertical DEP forces above the IDT electrodes with  $40 \mu\text{m}$  width and  $20 \mu\text{m}$  spacing. At the peak

voltage and frequency, the simulated vertical DEP force at the center of the  $5.4\ \mu\text{m}$  diameter (carboxyl coated) bead located on the oxide is about  $2.8 \times 10^{-14}\ \text{N}$  at  $1\ \text{V}_{\text{peak-to-peak}}$  and  $1\ \text{MHz}$ .

In case of the interaction between the bead and the unfunctionalized oxide surface, about  $1\ \text{V}_{\text{peak-to-peak}}$  was found to remove all beads located on the surface, as shown in Fig. 1(b). This can be analyzed as follows: The sedimentation or gravity force  $\mathbf{F}(4/3)\pi r^3(\rho_p - \rho_m)g$  ( $\sim 10^{-14}\ \text{N}$ ) acting on the center of the bead would cause the bead to move down toward the oxide surface, where  $r = 2.7 \times 10^{-6}\ \text{m}$  is the radius of the bead,  $g = 9.8\ \text{m/s}^2$  is the acceleration of gravity, and  $\rho_p = 1.05 \times 10^3\ \text{kg/m}^3$  and  $\rho_m = 1 \times 10^3\ \text{kg/m}^3$  are the densities of the bead and medium, respectively. Since the acid dissociation constants of the oxide surface and carboxyl molecule are 2–4 (Ref. 13) and 2.2,<sup>14</sup> the oxide surface and beads functionalized by the carboxyl group are usually negatively charged in a DI wafer at pH 7. Therefore, before the voltage is applied, there would be electrostatic repulsion forces between the negative charges on the bead and those on the oxide surface. There would also be an image force and van der Waals–London interaction between the bead and the unfunctionalized surface. As the bead is repelled away by the negative DEP and removed away from the surface, the electrostatic repulsion, the dipole-image force, and van der Waals–London forces can be ignored since these decrease as  $\propto 1/R^2$ ,  $\propto 1/(2R)^4$ ,<sup>15</sup> and  $\propto 1/R^7$ ,<sup>16</sup> respectively, where  $R$  is the distance between the bead and the oxide surface. Hence, the lift-off voltage where the bead is levitated at the equilibrium height can be calculated by finding the voltage at which the height balanced between the gravity and the simulated negative DEP force acting on the center of bead has changed significantly. From the calculated curve in Fig. 2(b), the voltage at which the equilibrium height changes significantly is around  $1\ \text{V}_{\text{peak-to-peak}}$ . This calculated value matches well with the voltage needed to experimentally remove all the beads from the center of the electrodes, as shown in Fig. 1(b). Hence, the simulation and experimental methodology presented here match each other quite well.

Using this methodology, we can also examine the interaction forces between the carboxyl functionalized bead and the poly-L-lysine functionalized surface using the DEP tweezers concept. L-lysine has two amino molecules and one carboxyl molecule, where the acid dissociation constants of the amino molecules and carboxyl molecule are 8.90, 10.28, and 2.20, respectively, and the isoelectric point is 9.59.<sup>14</sup> Hence, the net charge on the L-lysine molecule is  $+1.6 \times 10^{-19}\ \text{C}$  in the DI water (pH 7). Since the carboxyl group attached on the bead is negatively charged ( $-1.6 \times 10^{-19}\ \text{C}$ ) in the DI water, the main binding mechanism between the carboxyl and poly-L-lysine would be electrostatic attraction which is proportional to  $1/R^2$ . As expected and shown in Fig. 1(b) (squares), the lift-off voltage needed to remove the beads from the center of the electrodes is much higher and was measured to be about  $100\ \text{V}_{\text{peak-to-peak}}$ . This is due to the fact that electrostatic attractive forces must now be overcome by the vertical DEP force before the beads can be removed from the surface. At the voltage, the effect of the poly-L-lysine on the applied electric field can be ignored for the reason that the average diameters of poly-L-lysine with 18 amino groups or 78 amino groups are 31.5 and 40.5 nm, respectively.<sup>17</sup> As a first approximation, the length of L-lysine with two

amino groups is about 1.1–3.5 nm, resulting in the charge density ( $\rho_L$ ) of  $4.57 \times 10^{-11}$ – $1.45 \times 10^{-10}\ \text{C/m}$ . The electric field due to the poly-L-lysine can be calculated by  $d\mathbf{E} = (\rho_L dx / 4\pi\epsilon_{\text{DI}})[(z\hat{z} - x\hat{x}) / (x^2 + z^2)^{3/2}]$ ,<sup>18</sup> where  $z$  is located on the  $x$  axis,  $-20 \leq x \leq 20\ \mu\text{m}^2$  (the same width of the electrode) is the area where Poly-L-lysine is attached, and  $\epsilon_{\text{DI}}$  are the permittivity of DI water. The electric field generated by poly-L-lysine is about  $4.02 \times 10^3$ – $1.27 \times 10^4\ \text{V/m}$  at  $z = 2.7\ \mu\text{m}$ . The calculated electric field generated by  $100\ \text{V}_{\text{peak-to-peak}}$  with the electrode ( $-20 \leq x \leq 20\ \mu\text{m}$ ), about  $10^6\ \text{V/m}$  at  $z = 2.7\ \mu\text{m}$  and  $x = 0$ . Hence, the effect of electric field due to the charges of poly-L-lysine can be ignored. If we increase the input voltage from  $1\ \text{V}_{\text{peak-to-peak}}$  (negative DEP force =  $2.82 \times 10^{-14}\ \text{N}$ ) to  $100\ \text{V}_{\text{peak-to-peak}}$  (increase by  $10^2$ ), the DEP force is increased  $10^4$  times since the DEP force scales as  $V^2$ . Therefore, the estimated unbinding force for carboxyl coated beads would be about 280 pN. The unbinding force of streptavidin-biotin measured by AFM is about several hundreds of piconewtons as the function of pulling time,<sup>1</sup> and the unbinding forces of various antigen-antibody complexes ranges from several tens of piconewtons to several thousands of piconewton.<sup>3,4,7</sup> Our approach appears to be capable of measuring and estimating forces in the same range of forces.

In summary, in this study we demonstrated the concept of “DEP tweezers,” the main feature being that negative DEP force is used to remove a particle from a surface and the force needed to remove the particle can correlate to the strength of interaction between the particle and the surface. The simulated voltages to “lift off” the particles from the surface were close to the voltages obtained from experimental result on unfunctionalized surfaces. When oppositely charged beads and surfaces are used, the lift-off voltage required was higher than expected, proving that the measurement approach in general can be used for characterizing and examining the forces of interaction between various ligand-receptor pairs within microfluidic devices.

<sup>1</sup>G. U. Lee, D. A. Kidwell, and R. J. Colton, *Langmuir* **10**, 354 (1994).

<sup>2</sup>R. Tos, F. Schwesinger, D. Anselmetti, M. Kubon, R. Schafer, A. Pluckthun, and L. Tiefenauer, *Proc. Natl. Acad. Sci. U.S.A.* **95**, 7402 (1998).

<sup>3</sup>P. B. Chowdhury and P. F. Luckham, *Colloids Surf., A* **143**, 53 (1998).

<sup>4</sup>S. Wielert-Badt, P. Hinterdorfer, H. J. Gruber, J.-T. Lin, D. Badt, B. Wimmer, H. Schindler, and R. K.-H. Kinne, *Biophys. J.* **82**, 2767 (2002).

<sup>5</sup>K. Helmerson, R. Kishore, W. D. Phillops, and H. H. Weetall, *Clin. Chem.* **43**, 379 (1997).

<sup>6</sup>M. N. Liang, S. P. Smith, S. J. Metallo, I. S. Choi, M. Prentiss, and G. M. Whitesides, *Proc. Natl. Acad. Sci. U.S.A.* **97**, 13092 (2000).

<sup>7</sup>O. Bjornham, E. Fallman, O. Axner, J. Ohlsson, U. J. Nilsson, T. Boren, and S. Shedlin, *J. Biomed. Opt.* **10**, 044024 (2005).

<sup>8</sup>C. Gosse and V. Croquette, *Biophys. J.* **82**, 3314 (2002).

<sup>9</sup>F. Assj, R. Jenks, J. Yang, C. Love, and M. Prentiss, *J. Appl. Phys.* **92**, 5584 (2002).

<sup>10</sup>C.-H. Chiou, Z.-F. Tseng, and G.-B. Lee, *IEEE 17th International MEMS Conference (IEEE MEMS 2004)*, January 25–29, 2004, Maastricht, Netherlands, pp. 613–616.

<sup>11</sup>H. Li and R. Bashir, *Sens. Actuators B* **36**, 215 (2002).

<sup>12</sup>M. Washizu and T. B. Jones, *J. Electrostat.* **33**, 187 (1994).

<sup>13</sup>J. Tien, A. Terfort, and G. M. Whiteside, *Langmuir* **13**, 5349 (1997).

<sup>14</sup>[www.chemie.fu-berlin.de/chemistry/bio/aminoacid/lysine\\_en.html](http://www.chemie.fu-berlin.de/chemistry/bio/aminoacid/lysine_en.html)

<sup>15</sup>J.-H. J. Cho, B. M. Law, and F. Rieutord, *Phys. Rev. Lett.* **92**, 166102 (2004).

<sup>16</sup>F. London, *Trans. Faraday Soc.* **33**, 8 (1937).

<sup>17</sup>A. Harada and K. Kataoka, *Science* **283**, 65 (1999).

<sup>18</sup>D. K. Cheng, *Field and Wave Electromagnetics* 2nd ed. (Addison-Wesley, New York, 1989), Chap. 3.